In vivo evidence for cooperation of Mia40 and Erv1 in the oxidation of mitochondrial proteins

Lena Böttinger[a,b,*], Agnieszka Gornicka[c,*], Tomasz Czerwik[c], Piotr Bragoszewski[c], Adrianna Loniewska-Lwowska[c,†], Agnes Schulze-Specking[a], Kaye N. Truscott[d], Bernard Guiard[e], Dusanka Milenkovic[a,‡], and Agnieszka Chacinska[c]

[a]Institut für Biochemie und Molekularbiologie, Zentrum für Biochemie und Molekulare Zellforschung, and [b]Fakultät für Biologie, Universität Freiburg, 79104 Freiburg, Germany; [c]International Institute of Molecular and Cell Biology, 02-109 Warsaw, Poland; [d]Department of Biochemistry, La Trobe Institute for Molecular Science, La Trobe University, Melbourne, 3086, Australia; [e]Centre de Génétique Moléculaire, Centre National de la Recherche Scientifique, 91190 Gif-sur-Yvette, France

ABSTRACT **The intermembrane space of mitochondria accommodates the essential mitochondrial intermembrane space assembly (MIA) machinery that catalyzes oxidative folding of proteins. The disulfide bond formation pathway is based on a relay of reactions involving disulfide transfer from the sulfhydryl oxidase Erv1 to Mia40 and from Mia40 to substrate proteins. However, the substrates of the MIA typically contain two disulfide bonds. It was unclear what the mechanisms are that ensure that proteins are released from Mia40 in a fully oxidized form. In this work, we dissect the stage of the oxidative folding relay, in which Mia40 binds to its substrate. We identify dynamics of the Mia40–substrate intermediate complex. Our experiments performed in a native environment, both in organello and in vivo, show that Erv1 directly participates in Mia40–substrate complex dynamics by forming a ternary complex. Thus Mia40 in cooperation with Erv1 promotes the formation of two disulfide bonds in the substrate protein, ensuring the efficiency of oxidative folding in the intermembrane space of mitochondria.**

Monitoring Editor
Thomas D. Fox
Cornell University

Received: May 10, 2012
Revised: Aug 9, 2012
Accepted: Aug 14, 2012

INTRODUCTION

Proteins undergo various posttranslational modifications to reach their fully mature and functional forms. One of these modifications is the oxidation of cysteine residues and intermolecular or intramolecular disulfide bond formation to stabilize the structure or control the activity of a protein. In living cells disulfide bond formation is enzymatically catalyzed, and the major sites that accommodate the machineries responsible for disulfide bond formation are the endoplasmic reticulum of the eukaryotic cell and the bacterial periplasm (Riemer *et al.*, 2009; Bulleid and Elgaard, 2011; Depuydt *et al.*, 2011; Sato and Inaba, 2012). In these compartments the main players have been identified and characterized structurally, biochemically, and in a cellular context. The most recently discovered pathway for disulfide bond formation is the mitochondrial intermembrane space assembly (MIA) pathway in the intermembrane space of mitochondria (IMS), a compartment located between the outer and the inner mitochondrial membranes. An interesting and unique feature of this pathway is its function in the transport of proteins into the intermembrane space of mitochondria, which is indispensable for life (Hell, 2008; Chacinska *et al.*, 2009; Riemer *et al.*, 2009; Sideris and Tokatlidis, 2010). As for the vast majority of mitochondrial precursor proteins, the IMS precursors are transported across the outer mitochondrial membrane via the main entry gate, the translocase of the outer mitochondrial membrane (TOM) complex. After passage through the TOM complex, mitochondrial proteins follow specific pathways to submitochondrial destinations driven by the interplay between intrinsic signals within the precursors and their interaction with specific translocases (Dolezal *et al.*, 2006; Neupert and

This article was published online ahead of print in MBoC in Press (http://www.molbiolcell.org/cgi/doi/10.1091/mbc.E12-05-0358) on August 23, 2012.

*These authors contributed equally to this study.

Present addresses: †Medical Center for Postgraduate Education, 01-813 Warsaw, Poland; ‡Max Planck Institute for Biology of Ageing, 50931 Cologne, Germany.

The authors have no financial conflicts with regard to this study.

Address correspondence to: Agnieszka Chacinska (achacinska@iimcb.waw.pl).

Abbreviations used: GSH, glutathione; IMS, intermembrane space; MIA, mitochondrial intermembrane space assembly; MISS, mitochondrial intermembrane space sorting; TOM, translocase of the outer mitochondrial membrane.

Herrmann, 2007; Chacinska *et al.*, 2009). Intermembrane space proteins that are rich in cysteine residues arranged in the characteristic motifs CX_3C or CX_9C, such as the family of small Tim chaperones or copper ion–binding protein Cox17, respectively, are the classic substrates of the MIA pathway for oxidative folding (Koehler, 2004; Gabriel *et al.*, 2007; Khalimonchuk and Winge, 2008; Longen *et al.*, 2009). These proteins are initially recognized by Mia40, an essential protein in the MIA pathway (Chacinska *et al.*, 2004; Naoé *et al.*, 2004). Mia40 serves as a receptor at the *trans* side of the outer mitochondrial membrane that binds to the mitochondrial intermembrane space–sorting (MISS)/intermembrane space–targeting signal within precursors (Milenkovic *et al.*, 2009; Sideris *et al.*, 2009; von der Malsburg *et al.*, 2011). Because Mia40 is not only a receptor-like protein but also an oxidoreductase, the hydrophobic interactions between Mia40 and the MISS sequence within a substrate are strengthened by thiol–disulfide exchange, resulting in formation of an intermolecular disulfide bond between Mia40 and its substrate (Chacinska *et al.*, 2004; Grumbt *et al.*, 2007; Banci *et al.*, 2009, 2010; Kawano *et al.*, 2009; Milenkovic *et al.*, 2009; Tienson *et al.*, 2009). This disulfide-bonded Mia40–substrate conjugate constitutes the first critical intermediate step in the transport of the precursor into the IMS and transfer of disulfide bonds. On completion of disulfide bond transfer, the IMS proteins are released from Mia40 in the oxidized state (Mesecke *et al.*, 2005; Grumbt *et al.*, 2007; Müller *et al.*, 2008; Tienson *et al.*, 2009; Banci *et al.*, 2010). Mia40 contains six conserved cysteine residues found in the oxidized state, with the first two forming the redox-active CPC motif (Figure 1A; Mesecke *et al.*, 2005; Terziyska *et al.*, 2005; Chacinska *et al.*, 2008; Banci *et al.*, 2009; Kawano *et al.*, 2009). During the disulfide transfer reaction the cysteine residues of the Mia40 CPC motif become reduced. Another essential player, the sulfhydryl oxidase Erv1, is necessary to reoxidize the CPC motif of Mia40 (Mesecke *et al.*, 2005; Daithankar *et al.*, 2009; Bien *et al.*, 2010; Banci *et al.*, 2011). The MIA pathway shares similarities with other disulfide bond formation pathways. A common principle is a relay of thiol–disulfide exchange reactions and formation of intermolecular disulfide-bonded intermediate stages in these reactions, which mark separate events of disulfide transfer (Stojanovski *et al.*, 2008a; Riemer *et al.*, 2009). These functionally uncoupled events include 1) the passage of disulfide bonds from a disulfide carrier, Mia40 in the IMS, to a substrate and 2) the passage of disulfide bonds from a primary FAD-dependent oxidoreductase, such as Erv1 in the IMS, to a disulfide carrier, Mia40. Thus the relay concept implies that there is no contact between substrates and primary oxidoreductases.

However, the classic substrates of the MIA pathway adopt a hairpin-like structure stabilized by nonconsecutive disulfide bonds formed by the cysteine residues of CX_3C or CX_9C motifs (Arnesano *et al.*, 2005; Webb *et al.*, 2006; Baker *et al.*, 2009). We proposed earlier that the formation of two disulfide bonds in the small Tim proteins are mechanistically coupled and require Erv1 (Stojanovski *et al.*, 2008b). This proposal was based on a mechanistic dissection of oxidative folding steps in a substrate reconstituted in isolated mitochondria and a direct functional involvement of Erv1 in this process. The activity of Erv1 was suggested to be independent of reoxidation of the CPC motif in Mia40. These results led to the concept of a ternary complex in which both Mia40 and Erv1 cooperate in the transfer of multiple disulfide bonds to a substrate protein (Stojanovski *et al.*, 2008b). However, this idea was not supported by in vitro studies (Banci *et al.*, 2009, 2011; Terziyska *et al.*, 2009; Bien *et al.*, 2010). The reconstitution of the MIA oxidation pathway (or its single steps) with purified components resulted in the conclusion that Mia40 is able to drive complete oxidation of its substrates. Thus the mechanisms of substrate oxidation in the IMS remained controversial, leaving unanswered questions as to whether Erv1 contributes to this process.

In this work, the aim was to dissect the mechanistic requirements for oxidative protein biogenesis in the intermembrane space of mitochondria. We set up a novel assay in which saturating amounts of substrate protein were used. This assay allowed us to examine the changes in Mia40 upon precursor binding. Furthermore, by using the substrate proteins fused to affinity purification tags, we could address the involvement of Erv1 in Mia40-driven oxidation of substrates. We demonstrate that Erv1 transiently associates and acts at the level of the Mia40–substrate intermediate in a process of disulfide bond channeling in the IMS of mitochondria.

RESULTS

Characterization of the single-cysteine mutants of Mia40

Mia40 contains six conserved cysteine residues arranged in the CPC motif and twin CX_9C motif found in their oxidized forms (Figure 1A). Mia40 is essential for the viability of yeast, and therefore to generate yeast strains harboring mutant versions of the protein we performed plasmid shuffling. The genes encoding versions of Mia40 with various single amino acid substitutions of Cys to Ser—Mia40-C1S, Mia40-C2S, Mia40-C3S, Mia40-C4S, Mia40-C5S, and Mia40-C6S—and the wild-type Mia40 in the yeast plasmid were transformed into the strain harboring the deletion of MIA40 rescued by the MIA40-containing plasmid with the *URA3* marker. To check the phenotype of the yeast strains harboring the Mia40 cysteine mutants, we subjected the resulting transformants to a plasmid shuffling procedure upon treatment with 5-fluoroorotic acid. On this treatment the *URA3* plasmid carrying wild-type version of Mia40 was removed. No viable colonies were recovered for the strain bearing the Mia40-C2S mutant, pointing to an essential role of the second cysteine residue of Mia40 (Supplemental Figure S1A). The substitution of C6 in Mia40 resulted in a clear temperature-sensitive phenotype, whereas the substitution of C4 and C5 did not result in any detectable growth deficiency under the conditions tested (Figure 1B). The C1 and C3 mutants of Mia40 showed growth defects already at lower temperature (Figure 1B) but were viable, in contrast to previous reports (Kawano *et al.*, 2009; Terziyska *et al.*, 2009). However, the C1 and C3 Mia40 mutants did not grow on the respiratory carbon source at any temperature, as they lost functional mitochondrial DNA ($rho^{-/0}$; Figure 1B and unpublished data). To analyze the $rho^{-/0}$ strains harboring Mia40-C1S and Mia40-C3S, we generated the $rho^{-/0}$ versions of the wild-type strain, as well as Mia40-C6S strain. The analysis of steady-state levels of proteins revealed a major decrease in the levels of Tim10, a canonical substrate of the MIA pathway (Chacinska *et al.*, 2004; Stojanovski *et al.*, 2008b), in mitochondria from Mia40-C1S and Mia40-C3S strains, whereas a small reduction was observed in mitochondria from Mia40-C6 (Supplemental Figure S1B). In addition, an increase in the Mia40 levels in both Mia40-C1S and Mia40-C3S mutants and in levels of Erv1 in the case of Mia40-C3S mitochondria was observed (Supplemental Figure S1B). For comparison, mutants with Mia40-C4S and Mia40-C5S displayed a minor reduction in Tim10 levels, accompanied by minor variations in the levels of Mia40 and Erv1 (Supplemental Figure S1C). Other mitochondrial proteins were not affected (Supplemental Figure S1C). The importance of both C1 and C3 in Mia40 was further confirmed by the analysis of import and assembly of radioactively labeled Tim9, another protein of the small Tim family and a MIA substrate (Chacinska *et al.*, 2004; Koehler, 2004; Milenkovic *et al.*, 2009). Tim9 was imported into mitochondria isolated from the wild-type, Mia40-C1S, Mia40-C3S,

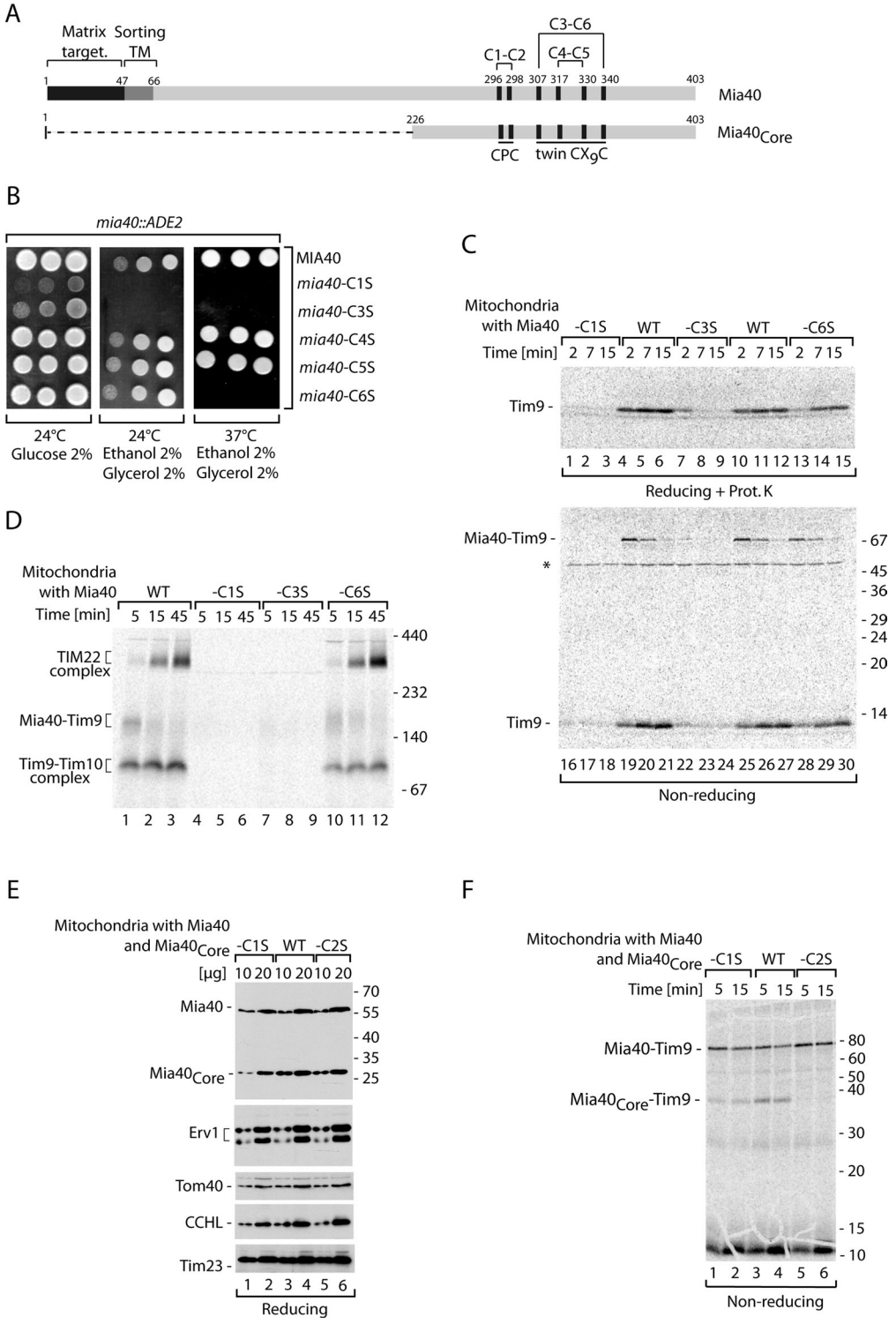

FIGURE 1: Single-cysteine-residue mutants of Mia40 show different growth phenotype and activity. (A) Schematic representation of Mia40 and its catalytic domain ($Mia40_{Core}$), showing localization of Cys residues and their arrangement in the motifs, as well as disulfide bonds formed between Cys residues. (B) The growth of yeast with wild-type Mia40, Mia40-C1S, Mia40-C3S, Mia40-C4S, Mia40-C5S, and Mia40-C6S. (C) The ^{35}S-labeled Tim9 was imported into mitochondria isolated from yeast with wild-type Mia40, Mia40-C1S, Mia40-C3S, or Mia40-C6S ($rho^{0/-}$ versions). Samples were treated with proteinase K when indicated and analyzed by nonreducing and reducing SDS electrophoresis as indicated. (D) Tim9 was imported into mitochondria isolated from yeast with wild-type Mia40, Mia40-C1S, Mia40-C3S, or Mia40-C6S ($rho^{0/-}$ versions). Mitochondrial extracts were lysed in digitonin and were separated by blue native electrophoresis. (E) The steady-state protein levels of mitochondria isolated from wild-type cells coproducing $Mia40_{Core}$, $Mia40_{Core}$-C1S, or $Mia40_{Core}$-C2S. Samples were analyzed by reducing SDS electrophoresis and immunodecoration. (F) Tim9 was imported into mitochondria isolated from wild-type cells coproducing $Mia40_{Core}$, $Mia40_{Core}$-C1S, or $Mia40_{Core}$-C2S. Samples were analyzed by reducing SDS electrophoresis. WT, wild type.

and Mia40-C6S strains devoid of functional mitochondrial DNA ($rho^{-/0}$). The import efficiency of Tim9 (Figure 1C, lanes 1–15), as well as formation of the covalent intermediate Mia40–Tim9 detected under nonreducing conditions (Figure 1C, lanes 16–30), was dramatically reduced in the Mia40-C1S and Mia40-C3S mitochondria and also partially reduced in mitochondria with Mia40-C6S. Tim9 imported into isolated mitochondria and analyzed under native conditions forms an intermediate with Mia40 before its oxidation, which is a prerequisite for assembly into the mature hexameric Tim9–Tim10 complex and the TIM22 translocase complex (Chacinska *et al.*, 2004; Müller *et al.*, 2008; Stojanovski *et al.*, 2008b). As expected, Mia40-C1S and Mia40-C3S were unable to efficiently engage with the Tim9 precursor, resulting in the absence of the mature assembled complexes (Figure 1D). The import analysis indicated that mitochondria with Mia40-C5S and Mia40-C4S were partly defective in import of Tim9 (Supplemental Figure S1D, lanes 1–15) and in formation of the disulfide-bonded intermediate between Mia40 and Tim9 (Supplemental Figure S1D, lanes 16–30).

The importance of the C2 residue in Mia40 has been already described on the basis of its essential role for growth and also on the basis of in vitro biochemical characterization using purified proteins (Kawano *et al.*, 2009; Terziyska *et al.*, 2009). To check the effect of substituting C2 with Ser in the native environment of mitochondria, we constructed yeast strains in which the conserved region of Mia40, $Mia40_{Core}$, was coexpressed from the plasmid in addition to the genome-expressed wild-type Mia40. $Mia40_{Core}$, although much smaller than the wild-type protein (Figure 1A), can substitute for the function of wild-type Mia40 (Chacinska *et al.*, 2008). In addition to $Mia40_{Core}$ with all the cysteine residues intact, we produced the strains expressing $Mia40_{Core}$ with C1 or C2 changed to Ser. These two versions of $Mia40_{Core}$ accumulated in mitochondria as efficiently as did wild-type $Mia40_{Core}$, and in addition the levels of other tested mitochondrial proteins did not differ (Figure 1E). We imported Tim9 into the isolated mitochondria and analyzed these reactions under nonreducing conditions for the formation of the Mia40–Tim9 intermediate (Figure 1F). $Mia40_{Core}$-C2S did not bind Tim9, whereas $Mia40_{Core}$-C1S did but with reduced efficiency as compared with the wild-type version of $Mia40_{Core}$. Glutathione (GSH) was reported to increase the efficiency of import and formation of Mia40–substrate conjugates by performing the proofreading function in the MIA pathway (Bien *et al.*, 2010). We tested how the $Mia40_{Core}$-C1S and $Mia40_{Core}$-C2S react in the presence of GSH (Supplemental Figure S1E). We observed an improvement in the Mia40-Tim9 intermediate formation in the presence of physiological concentrations of GSH and inhibition in the presence of GSH excess, as expected for wild-type mitochondria (Bien *et al.*, 2010) and for mitochondria with $Mia40_{Core}$-C1S (Supplemental Figure S1E). It remains puzzling what is the source of oxidizing power for Mia40-C1S (lacking the oxidized CPC motif) to form conjugates with the IMS precursors. In addition to the possibility that C2 would be engaged in another disulfide bond within the Mia40 molecule, another scenario is that C2 of Mia40 can be glutathionylated. GSH did not influence the $Mia40_{Core}$-C2S inability to bind Tim9 (Supplemental Figure S1E).

In summary, by testing the role of the entire set of Mia40 cysteine residues in vivo by growth and the ability to bind and import the IMS precursors in the native environment of mitochondria, we could assign the relative importance of the Mia40 cysteine residues. Our analysis demonstrated that C2 of Mia40 is absolutely necessary for the formation of the intermolecular disulfide bond with protein substrates. This agrees well with data derived from purified proteins (Banci *et al.*, 2009; Kawano *et al.*, 2009; Terziyska *et al.*, 2009). In this analysis both Mia40-C1 and Mia40-C3 mutants displayed a very similar phenotype and functional characteristics. C1 and C3 of Mia40 were not essential for life but seemed to play an important and related role. The C6 residue of Mia40, although less important than C1 or C3, was functionally relevant, as highlighted by the temperature-sensitive phenotype and biochemical characterization of Tim9 import into mitochondria. C4 and C5 of Mia40 were found to be dispensable for efficient growth; however, C5 was important for efficient import of Tim9. This analysis raises the possibility that the C3 and C6 pair also plays a role in oxidation of substrate proteins.

Mia40 undergoes redox-conformational changes upon precursor binding

We set up an assay to assess changes in Mia40 upon precursor binding. Recombinant $Tim12_{His}$ was purified from *Escherichia coli* and imported into isolated mitochondria. In contrast to radiolabeled precursors (Figure 1; Chacinska *et al.*, 2004; Stojanovski *et al.*, 2008b; Milenkovic *et al.*, 2009), we could manipulate the amount of precursor to saturate Mia40 and detect putative changes in Mia40 using specific antibodies. We used mitochondria isolated from the strain that coproduced both wild-type Mia40 and plasmid-borne $Mia40_{Core}$. When we imported $Tim12_{His}$, we observed an efficient shift of both Mia40 versions to the higher–molecular weight range (Figure 2A). These new species likely corresponded to Mia40 engaged with the Tim12 substrate, since they were recognized by the Mia40-specific antibody and did not appear in the mock control (no precursor added; Figure 2A, lane 4). The intermediate stages represented the disulfide-bonded conjugates, as they diminished after treatment with the reducing agent (Figure 2A, lanes 5–8). Of interest, not only was one Mia40 intermediate visible, as was frequently the case for the radioactively labeled precursors, but so were at least three distinct stages of Mia40. This raised a concern that some of the species represented Mia40 released from the Tim12 substrate. To address this possibility, we performed a pull-down experiment. After import of $Tim12_{His}$, mitochondria were solubilized with digitonin and extract was loaded onto nickel-nitriloacetic acid (Ni-NTA) agarose and analyzed under nonreducing conditions. A set of Mia40–Tim12 intermediates was detected in the load fraction (Figure 2B, lanes 1–3). The same set of intermediates was highly enriched in the elution fraction (Figure 2B, lanes 5–7). This demonstrates that the species formed upon $Tim12_{His}$ import represent conjugates with Mia40. Next we performed the import reaction in the presence of GSH (Figure 2C), which was shown to reduce the off-pathway intermediates of Mia40 (Bien *et al.*, 2010). GSH added at physiological concentrations did not change the pattern and quantity of the intermediate formation between Mia40 and recombinant substrate $Tim12_{His}$ (Figure 2C). Thus none of the protein species behaved as an off-pathway product.

We titrated the amount of imported $Tim12_{His}$ to assess saturation of the Mia40–Tim12 intermediate formation and depletion of the free Mia40 pool. We observed Mia40 depletion and efficient Mia40–Tim12 formation even with low concentrations of $Tim12_{His}$ substrate (Supplemental Figure S2A). To exclude the possibility that the formation of a complex pattern of Mia40–substrate intermediates is specific only for $Tim12_{His}$, we used another recombinant precursor, $Tim10_{His}$. On import of $Tim10_{His}$, we observed generation of two species, which increased in response to the increasing amount of $Tim10_{His}$, resulting in depletion of free Mia40 (Supplemental Figure S2B). Thus, to reach Mia40 saturation, more $Tim10_{His}$ than $Tim12_{His}$ was needed. However, when $Tim10_{His}$ was tested in a time-dependent kinetics, it formed a similar set of intermediate conjugates with Mia40 (Figure 2D).

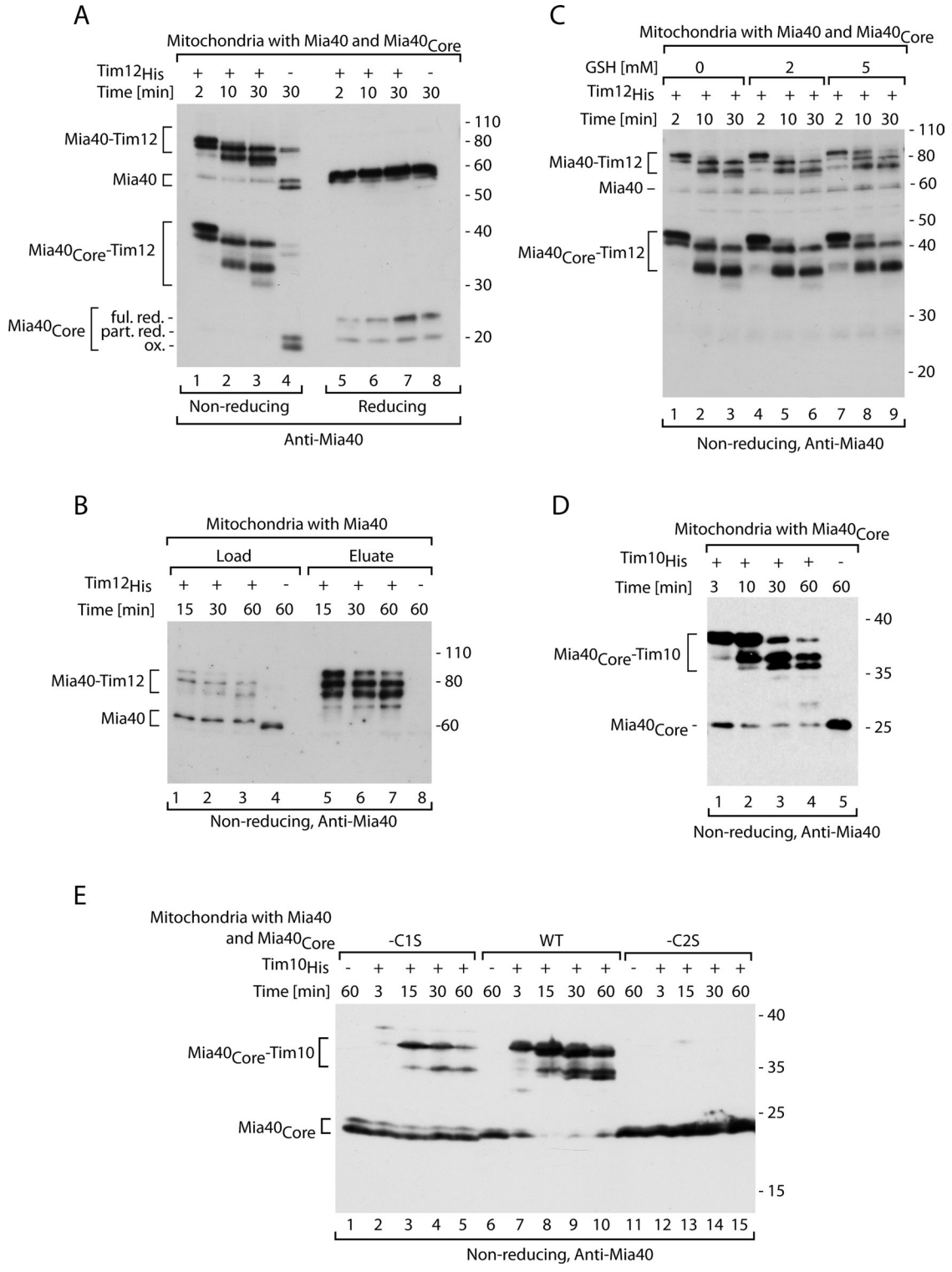

FIGURE 2: Characterization of the intermediates formed by recombinant small Tim proteins and Mia40. (A) $Tim12_{His}$ was imported into mitochondria isolated from wild-type cells coproducing $Mia40_{Core}$ and analyzed by immunodecoration with Mia40. Ful. red., fully reduced; ox., oxidized; part. red., partially reduced. (B) Affinity purification of $Tim12_{His}$ was performed after import into mitochondria and solubilization with digitonin. Load, 10%; eluate, 100%. (C) $Tim12_{His}$ was imported into mitochondria isolated from wild-type cells coproducing $Mia40_{Core}$ in the presence of increasing concentrations of GSH. (D) $Tim10_{His}$ was imported into mitochondria isolated from yeast cells expressing $Mia40_{Core}$. (E) $Tim10_{His}$ was imported into mitochondria isolated from wild-type (WT) cells coproducing $Mia40_{Core}$, $Mia40_{Core}$-C1S, or $Mia40_{Core}$-C2S. (A–E) Samples were analyzed by SDS electrophoresis and immunodecoration with anti-Mia40 serum.

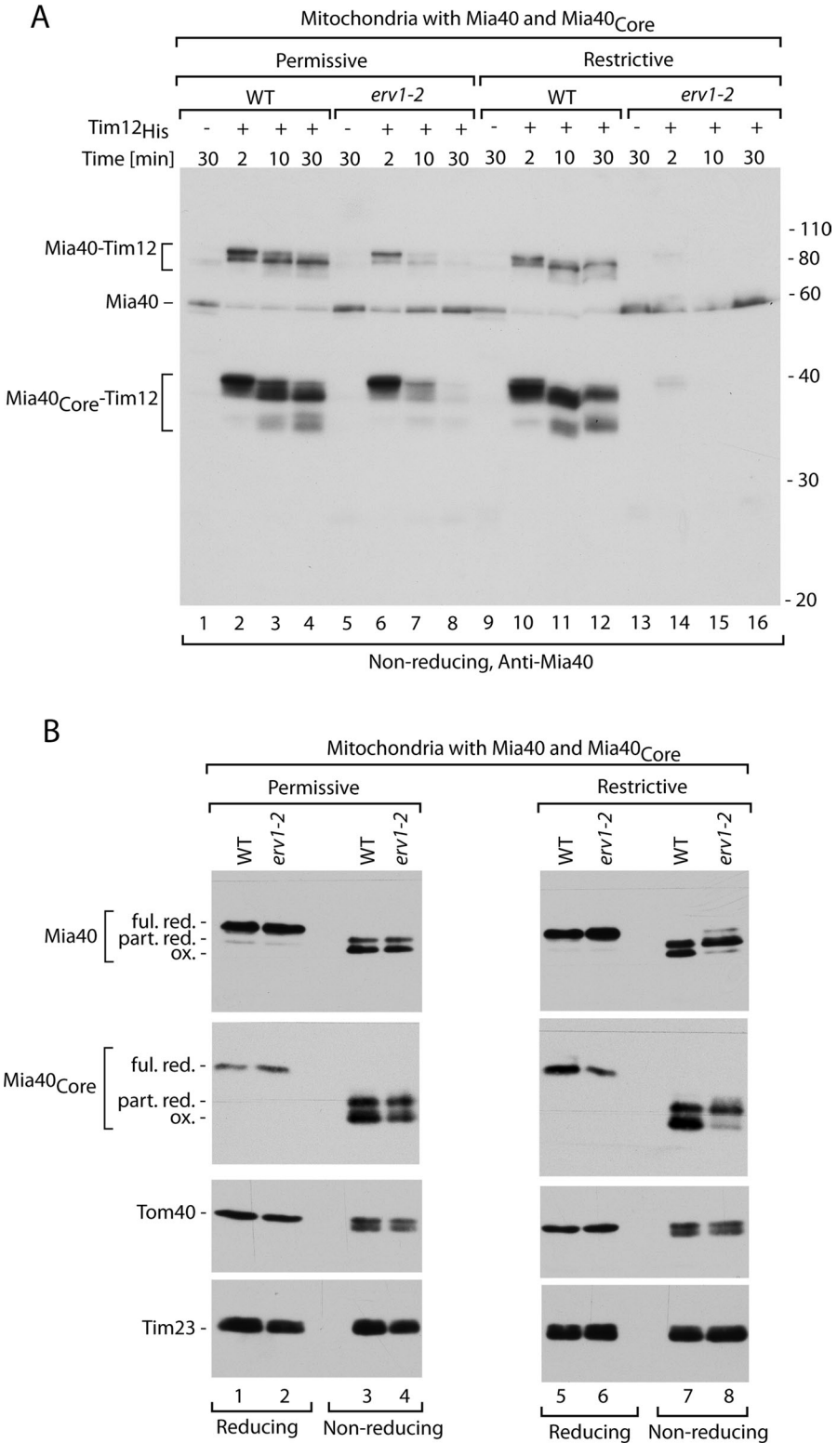

FIGURE 3: Formation of Mia40–substrate intermediates is affected in *erv1* mutant. (A) $Tim12_{His}$ was imported into mitochondria isolated under permissive (19°C) or restrictive (26°C) conditions from wild-type (WT) or *erv1-2int* cells coproducing $Mia40_{Core}$. Samples were analyzed by nonreducing SDS electrophoresis and immunodecoration with anti-Mia40 serum. (B) Redox state of Mia40 and $Mia40_{Core}$. Wild-type (WT) and *erv1-2int* mitochondria were subjected to denaturation in the presence of the reducing agent DTT (reducing) or the thiol-blocking agent iodoacetamide (nonreducing) at 60°C. Samples were analyzed by SDS electrophoresis and immunodecoration for Mia40 and control mitochondrial proteins as indicated. Ful. red., fully reduced; ox., oxidized; part. red., partially reduced.

To ensure the specificity of the observed Mia40 species, we analyzed the formation of Mia40–Tim10 intermediates in the $Mia40_{Core}$-C1S and $Mia40_{Core}$-C2S mutants produced in the background of wild-type Mia40 (Figure 2E). In agreement with the analysis with radioactive precursors (Figure 1F), this experiment demonstrated that C2 of Mia40 is necessary for binding and intermediate formation with recombinant substrate (Figure 2E, lanes 12–15). The $Mia40_{Core}$-C1S mutant was able to bind recombinant $Tim10_{His}$, albeit with reduced efficiency (Figure 2E, lanes 2–5). Thus we observed a set of specific intermediates between Mia40 and its substrates formed under the conditions of Mia40 saturation. These Mia40–precursor intermediates may reflect a dynamic behavior likely representing redox-conformational changes of Mia40–substrate in the transfer of disulfide bonds.

The redox-conformational changes of Mia40 upon substrate binding require Erv1

When we imported $Tim12_{His}$ into mitochondria isolated from the strain *erv1-2* grown under permissive conditions, we observed efficient formation of the early intermediate, although the next stages were inhibited (Figure 3A, lanes 1–8). Thus, under these conditions the initial binding of the substrate to Mia40 in the *erv1-2* background was similar to wild type, but the Mia40–substrate intermediate could not proceed to further stages. The lack of an initial binding defect correlated well with the unchanged redox state of Mia40 in *erv1-2* mitochondria compared with wild type (Figure 3B, lanes 1–4). This observation indicated a kinetic involvement of Erv1 in Mia40–substrate dynamics under permissive conditions. When we imported $Tim12_{His}$ into mitochondria isolated from the *erv1-2* strain grown under restrictive conditions, we observed no binding of Mia40 to the substrate (Figure 3A, lanes 9–16). This was in agreement with the redox state of Mia40, which adopted a partially reduced form in the *erv1-2* mitochondria (Figure 3B, lanes 5–8), representing reduction of the CPC motif (Mesecke *et al.*, 2005; Grumbt *et al.*, 2007). The control proteins, Tom40 and Tim23, remained unchanged (Figure 3B). These results based on the direct monitoring of Mia40 behavior agree well with previous results obtained from the analysis of substrate oxidation (Stojanovski *et al.*, 2008b).

The dynamics of Mia40 upon precursor binding and its dependence on Erv1 supported the functional involvement of Erv1 (Figures 2 and 3). However, we could not detect a species that represented Erv1 associated with Mia40–substrate in the ternary complex in our analysis under nonreducing

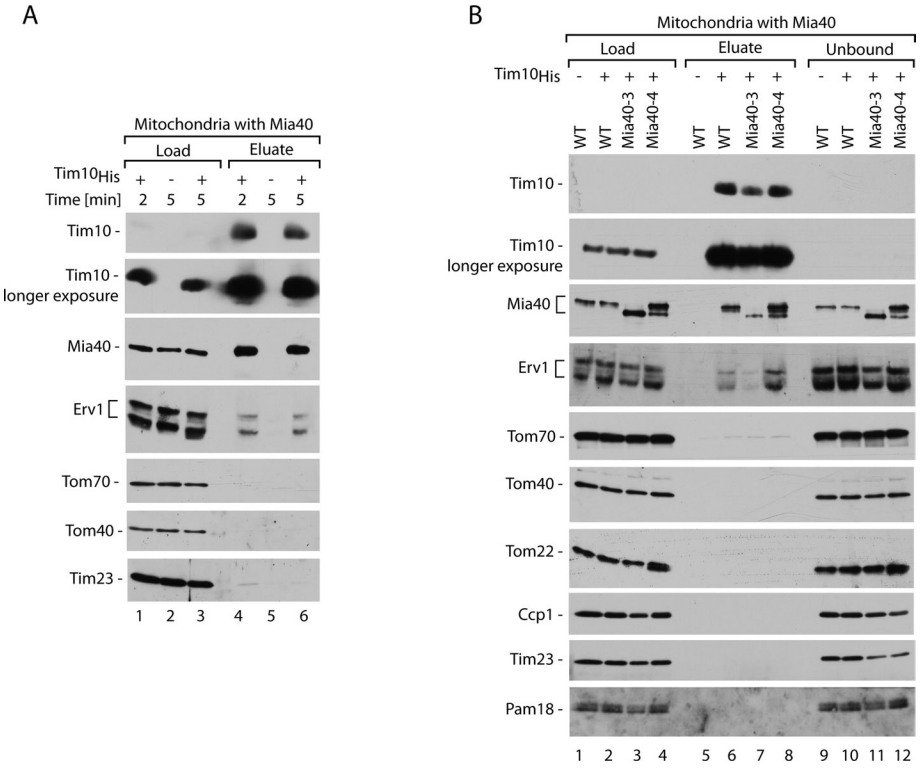

FIGURE 4: Erv1 is found in the eluate with small Tim proteins. (A) Ni-NTA affinity purification of $Tim10_{His}$ was performed upon import into mitochondria at 15°C and solubilization with digitonin. Load, 3%; eluate, 100%. (B) Ni-NTA affinity purification of $Tim10_{His}$ was performed upon import into mitochondria with wild-type (WT) Mia40, Mia40-3, or Mia40-4 for 3 min at 15°C, followed by solubilization with digitonin. Load, 3%; eluate, 100%. In A and B, samples were analyzed by reducing SDS electrophoresis and immunodecoration with different antisera as indicated. WT, wild type.

conditions (unpublished data). The ternary complex could be a very fast step, difficult or impossible to observe in our assays based on the detection of disulfide-bonded species. To directly assess the physical association of Erv1, we performed pull-down experiments with recombinant substrates in the course of their import into isolated mitochondria. Mitochondria with imported $Tim10_{His}$ were solubilized with digitonin, which preserves mild noncovalent protein interactions between $Tim10_{His}$ and its partners, and analyzed under reducing conditions (Figure 4A). $Tim10_{His}$ was efficiently purified (Figure 4A, lanes 4–6). In agreement with the previous experiment with $Tim12_{His}$ (Figure 2B), Mia40 was found in the eluate of $Tim10_{His}$, confirming the efficient formation of the Mia40–Tim10 intermediates. Of interest, the eluate of $Tim10_{His}$ also contained Erv1. The signal of Erv1 was not present in the eluate derived from mitochondria subjected to mock import without the recombinant substrate, demonstrating the specificity of this reaction (Figure 4A, lane 5). The control proteins, such as the outer membrane translocase components Tom40 and Tom70 and the inner membrane translocase component Tim23, were not eluted in this reaction (Figure 4A). It is interesting to note that Tim10 passes through the TOM complex as a main entry gate to mitochondria to reach Mia40 (Kurz *et al.*, 1999; Lutz *et al.*, 2003; von der Malsburg *et al.*, 2011); however, the interaction of Tim10 with TOM is either too transient or unstable to be detected in this assay. In summary, this finding demonstrates the direct involvement of Erv1 in the oxidation reaction of the Tim10 substrate. Erv1 associates with the imported recombinant precursor and participates in the dynamics of Mia40 upon precursor binding.

The question remained whether Erv1 binds to the imported precursor directly and independently of Mia40 or whether the binding of precursor to Mia40 is a prerequisite for Erv1 involvement. To answer this question, we used the two well-characterized conditional mutant strains *mia40-3* and *mia40-4* (Chacinska *et al.*, 2004; Müller *et al.*, 2008; Stojanovski *et al.*, 2008b). Mia40-3 does not bind the substrate proteins efficiently, whereas Mia40-4 binds the substrates but is defective in the subsequent step of release of the fully oxidized precursor. Thus the intermediate of Mia40–Tim10 is formed with a reduced efficiency in *mia40-3* and increased efficiency in *mia40-4* mutant mitochondria. Import of recombinant $Tim10_{His}$ into the mitochondria with Mia40-3 and Mia40-4 mutants was followed by affinity purification (Figure 4B). Indeed, various amounts of Mia40 were found in the eluate of $Tim10_{His}$ in the case of wild-type, Mia40-3, and Mia40-4 mitochondria, as expected based on the mutants' characteristics. The elution profile of Erv1 was very similar to that observed for Mia40 (Figure 4B); almost no Erv1 was present in the eluate from mitochondria with Mia40-3, whereas a significant increase was observed in the eluate from Mia40-4 mitochondria relative to wild-type mitochondria. Altogether, an intermediate complex formed by Mia40 and Tim10 is a binding partner of Erv1, which in turn promotes the transition of Mia40–Tim10 to the next stage of oxidative folding.

An alternative binding site for Erv1 at Mia40

Our analysis of the Mia40 cysteine mutants underscored a similarity between phenotypes of the mutants with substituted C1 and C3 (Figure 1 and Supplemental Figure S1). To address the role of these cysteine residues in formation of a ternary complex, we subjected mitochondria with Mia40-C1S and Mia40-C3S to recombinant $Tim10_{His}$ import and affinity purification. Given that the amounts of mutant versions were increased in mitochondria due to an unknown compensatory mechanism (Supplemental Figure S1 and Figure 5A, lanes 3 and 4), Mia40-C1S and Mia40-C3S came down less enriched in the eluate of recombinant $Tim10_{His}$ compared with wild-type Mia40 (Figure 5A, compare lanes 6–8 with lanes 2–4), as expected based on the defective substrate binding of these mutant versions of Mia40 (Figure 1). In general, the Erv1 binding efficiency was reduced in the $rho^{0/-}$ mitochondria compared with the earlier experiments (see Figure 4), likely due to a different metabolic state of these strains (lack of functional mitochondrial DNA). However, we noticed an increased appearance of Erv1 in the eluate derived from the mitochondria with Mia40-C3S (Figure 5A). To exclude the possibility that Mia40-C3S, due to its binding defect, was not saturated by $Tim10_{His}$, we performed affinity purifications with increasing amounts of $Tim10_{His}$ (Supplemental Figure S3). In contrast to increasing amount of $Tim10_{His}$, the pull-down of Mia40 did not improve (Supplemental Figure S3), demonstrating the complete saturation of Mia40-C3S. In summary, we concluded that in mitochondria with

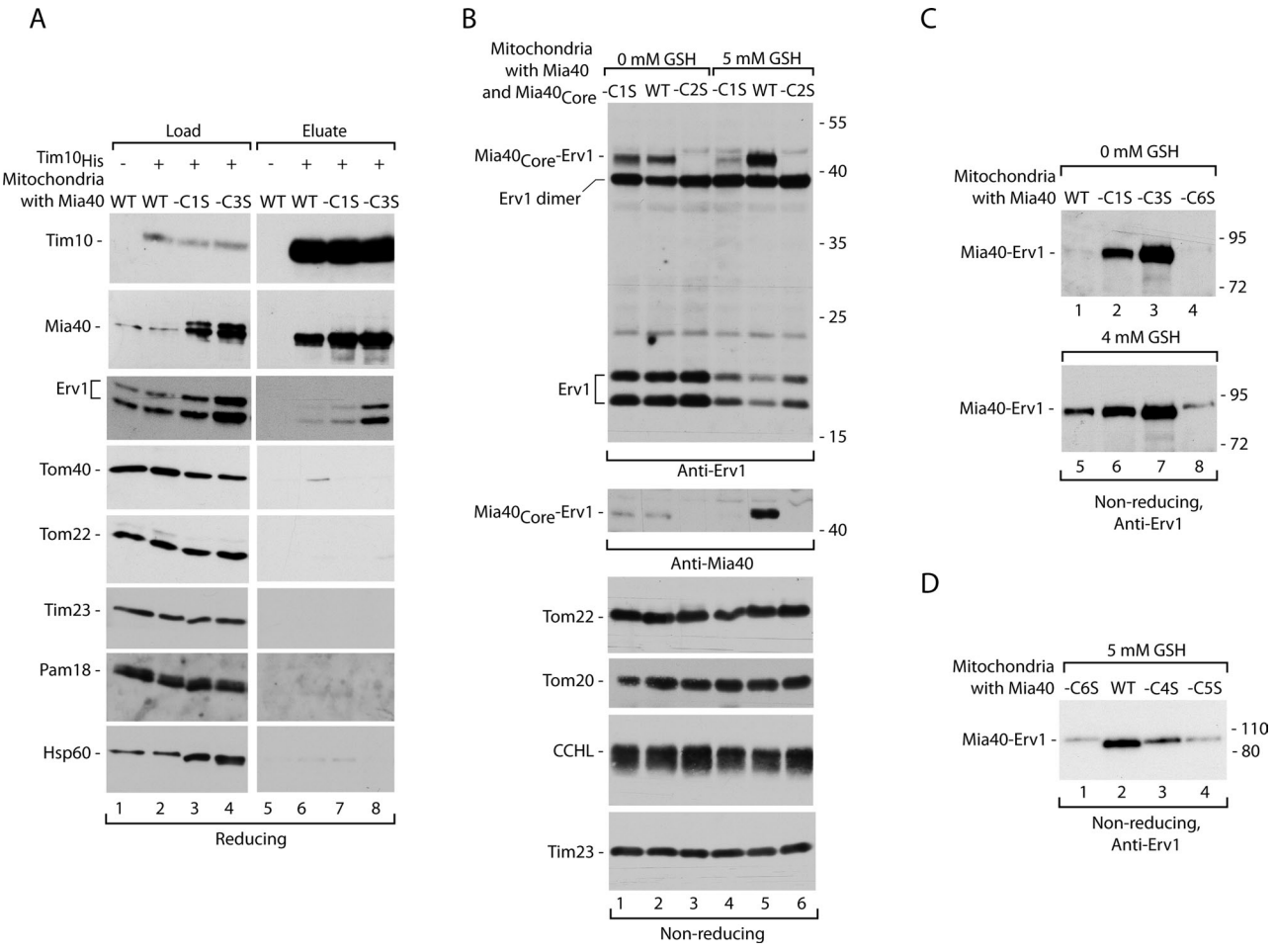

FIGURE 5: Single cysteine residue mutants of Mia40 differ in Mia40-Erv1 complex formation. (A) Ni-NTA affinity purification was performed upon import of $Tim10_{His}$ into mitochondria with wild-type (WT) Mia40, Mia40-C1S, or Mia40-C3S, followed by solubilization with digitonin. Load, 3%; eluate, 100%. (B) Mitochondria isolated from wild-type cells coproducing $Mia40_{Core}$ (WT), $Mia40_{Core}$-C1S, or $Mia40_{Core}$-C2S were subjected to GSH treatment. (C) Mitochondria isolated from yeast with Mia40 (WT), Mia40-C1S, Mia40-C3S, or Mia40-C6S (rho$^{0/-}$ versions) were subjected to GSH treatment. (D) Mitochondria with Mia40 (WT), Mia40-C4S, Mia40-C5S, or Mia40-C6S were subjected to GSH treatment. In A–D, samples were analyzed by reducing or nonreducing SDS electrophoresis and immunodecoration with different antisera as indicated.

Mia40-C3S the ternary complex is stabilized (Figure 5A). This increase in the ternary complex formation is difficult to explain by only an increase in the steady-state levels of Erv1 in the Mia40-C3S mitochondria (Supplemental Figure S1), as in this assay we purified species that are bound to substrate during its oxidative folding.

To further examine the binding of Erv1 to Mia40 in the absence of precursors, we used the strain that produces two versions of Mia40, wild type and $Mia40_{Core}$ (Figure 1A). Isolated mitochondria were incubated with an increased concentration of GSH (albeit not higher than physiological). Addition of GSH resulted in stabilization of the band recognized by both Mia40- and Erv1-specific antisera (Supplemental Figure S4A). The size of the bands (~50 kDa for mitochondria with $Mia40_{Core}$ and 80 kDa for Mia40) roughly corresponded to the sum of molecular weights of $Mia40_{Core}$ (25 kDa) or native Mia40 (migration 55 kDa) with Erv1 (23 kDa). Thus we identified protein complexes representing the conjugates of Mia40 and Erv1 (Supplemental Figure S4A). Erv1, similar to Mia40 substrates, was found to bind to C2 of the CPC motif in Mia40, as revealed by experiments with purified components (Terziyska *et al.*, 2009; Banci *et al.*, 2011). It was concluded that this binding was necessary for Mia40 reoxidation. We tested Mia40-C1S and Mia40-C2S for their ability to bind Erv1 in intact mitochondria. The C1 mutant of Mia40 was found to bind Erv1 better than wild-type Mia40 (Figure 5B), but GSH did not lead to the stabilization of this interaction. In agreement with earlier data (Terziyska *et al.*, 2009; Banci *et al.*, 2011), in addition to its essential role in substrate binding, C2 is also important for Erv1 association in the absence of a substrate (Figure 4B). However, in our affinity purifications via a substrate (Figures 4 and 5A), we analyzed the species in which the C2 binding site for Erv1 at Mia40 was obviously occupied by the Tim10 substrate. Thus the alternative model of Mia40 association, either with Erv1 or substrate, was impossible to envisage in this experimental setup. Taken together, these results raise the possibility that there is an alternative Erv1-binding site on Mia40 that is uncovered by binding of a substrate to Mia40.

Of interest, Mia40-C3S was found to bind Erv1 better than wild type and even better than Mia40-C1 in the absence of a substrate (Figure 5C). These Erv1–Mia40 conjugates diminished upon treatment with reductant dithiothreitol (DTT; Supplemental Figure S4B). Erv1 was efficiently pulled down upon $Tim10_{His}$ substrate import in

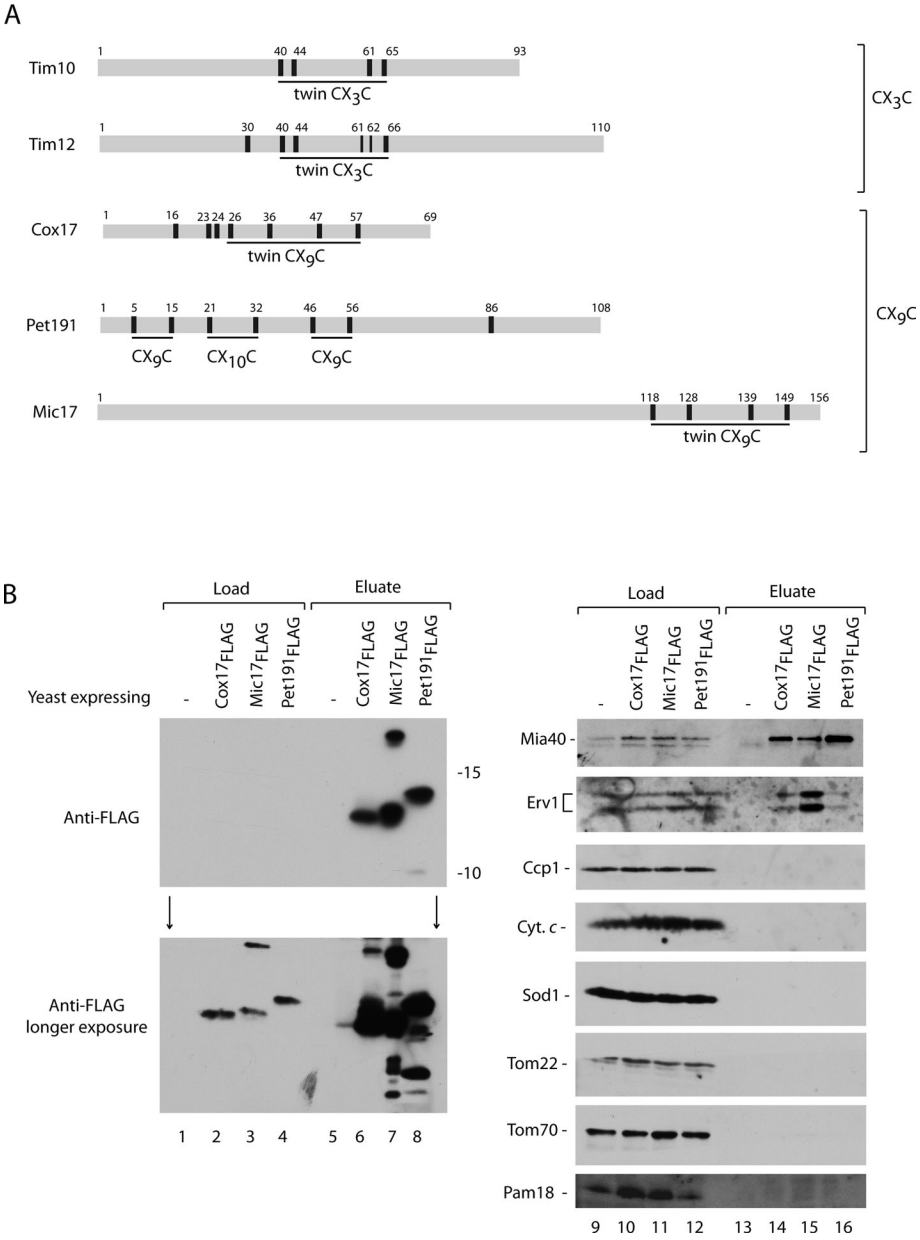

FIGURE 6: Mia40 and Erv1 copurify with IMS proteins in vivo. (A) Schematic representation of different MIA substrates classes. Localization of cysteine residues is indicated with black bars and numbers. The cysteine-rich motifs are underlined. (B) Anti-FLAG agarose affinity purification of $Cox17_{FLAG}$, $Mic17_{FLAG}$, or $Pet191_{FLAG}$ upon disruption and solubilization with digitonin of total yeast cells. Samples were analyzed by reducing SDS electrophoresis and immunodecoration with different antisera. Load, 5%; eluate, 100%.

mutant mitochondria harboring Mia40-C3S and also those harboring Mia40-4 (Figures 4B and 5A). We wondered whether this behavior correlated with an ability to form a conjugate between Mia40 and Erv1 without the involvement of a substrate. Indeed, similar to Mia40-C3S, Mia40-4 also displayed a prolonged interaction with Erv1 (Supplemental Figure S4C). The substitution of C3 to Ser leaves C6 in the reduced state, and Mia40-C6S was unable to bind to Erv1 efficiently (Figure 5, C and D). The increase of Erv1 binding typical for Mia40-C3 was not observed for the versions of Mia40 with Cys residues engaged with other disulfide bonds formed by the twin CX_9C motif, C4–C5 (Figure 5D). The differential effects observed for single C3 and C6 substitutions in Mia40 suggest that the C3–C6 pair participates in creation of an additional contact site for Erv1 at Mia40 used in the ternary complex.

The ternary complex is formed in vivo with various MIA substrates

All the data obtained so far with isolated mitochondria supported the redox-conformational dynamics of Mia40 with Erv1 involvement in oxidative folding of the IMS proteins. However our conclusions do not agree with the conclusions derived from in vitro reconstitution with the purified components and structural data (Bien *et al.*, 2010; Banci *et al.*, 2011). The discrepancy in mechanistic conclusions may originate from use of different assays (in vitro vs. in organello) and/or different precursors. Thus we decided to address the question of Erv1 involvement by using various types of precursors in an assay that mimicked well the situation in the cellular context. To this point classic precursors with twin CX_3C motifs belonging to the small Tim family (Figure 6A) were used in the assays with the isolated mitochondria. We chose representatives of the other classic MIA substrate family, which share twin CX_9C motifs: Cox17, Pet191, and Mic17 (Figure 6A; Gabriel *et al.*, 2007, Longen *et al.*, 2009). We generated the constructs coding for Cox17, Pet191, and Mic17 fused to a FLAG tag at their C-terminus and placed under the control of a strong and inducible *GAL10* promoter. The wild-type strain was transformed with the plasmids, and the yeast were grown on galactose to induce the production of fusion proteins (Supplemental Figure S5A). The expression of $Pet191_{FLAG}$ was checked after various induction times by the analysis of total protein extracts immunodecorated with the Pet191-specific antibodies (Supplemental Figure S5B, lanes 1–8). $Pet191_{FLAG}$ was efficiently induced already after 1 h of growth on galactose, as indicated by the protein band recognized by the specific antibody, which was absent in yeast cells transformed with empty plasmid (Supplemental Figure S5B, lanes 1–8). Two other proteins, $Mic17_{FLAG}$ and $Cox17_{FLAG}$, required a longer time for efficient induction (Supplemental Figure S5B, lanes 9–20).

All three fusion proteins were expressed and total cellular protein extracts prepared in the presence of mild detergent digitonin to preserve noncovalent and weak protein interactions. These extracts were subjected to the affinity purification using anti-FLAG agarose (Supplemental Figure S5A). The FLAG fusions were found in the eluate (Figure 6B, lanes 6–8). Only after overexposure did the FLAG signals in the load fractions became visible, demonstrating the high enrichment of the FLAG fusion proteins in the eluate (Figure 6B, lanes 2–4). In agreement with the in organello data (Figure 4), we observed an efficient interaction of the fusion proteins with Mia40 (Figure 6B, lanes 9–16). Furthermore, the Erv1

signal was also present in the eluate of all three fusion proteins. The interaction profile was strikingly similar to the results obtained with the substrate imported into isolated mitochondria (Figure 4). The efficiency of the pull-down for Erv1 was smaller compared with Mia40, suggesting a more transient interaction (Figure 6B, compare lanes 10–12 with lanes 14–16). The only clear exception to this pattern was the eluate derived from cells expressing $Mic17_{FLAG}$, in which Erv1 was found to be highly enriched. Thus Mic17 constitutes an interesting example of a substrate in which the transient ternary complex stage was prolonged compared with other substrates. Other mitochondrial proteins tested did not interact with the FLAG fusion proteins, showing the specificity of these interactions (Figure 6B, lanes 9–16). In summary, we demonstrated that in addition to small Tim proteins, other substrates of the MIA pathway also form a ternary complex with Mia40 and Erv1 during their oxidative folding. It was possible to detect the ternary complex in the native cellular context.

DISCUSSION

The MIA pathway is the most recently identified pathway responsible for thiol–disulfide exchange reactions and oxidative biogenesis of proteins. This pathway operates in the IMS of mitochondria. The mechanisms of protein oxidation in the IMS of mitochondria are not fully understood. A highly debated issue in the field is the relationship of Erv1 to Mia40 in the course of substrate oxidation. Mature proteins of the IMS contain multiple, typically two, nonconsecutive disulfide bonds. Oxidative folding is initiated by the engagement of substrate with Mia40 via a disulfide bond (Chacinska *et al.*, 2004; Grumbt *et al.*, 2007; Banci *et al.*, 2009, 2010; Milenkovic *et al.*, 2009). For this interaction the oxidizing power comes from the CPC motif of Mia40. When the single disulfide bond is passed to a substrate, the CPC motif of Mia40 becomes reduced, and Mia40 requires the activity of the FAD-dependent sulfhydryl oxidase Erv1 to reoxidize its CPC motif for the next round of disulfide transfer (Mesecke *et al.*, 2005; Banci *et al.*, 2011). This elegant model of a disulfide relay is similar to the protein oxidation mechanisms observed in the endoplasmic reticulum and bacterial periplasm (Stojanovski *et al.*, 2008a; Riemer *et al.*, 2009). Surprisingly, the conditional *erv1* mutants grown under permissive conditions did not show a defect in the formation of Mia40–substrate intermediate due to the intact and oxidized CPC motif; however, under these conditions they were defective in completion of substrate oxidation (Stojanovski *et al.*, 2008b). These findings raised a possibility that Erv1 may perform a catalytic function in this process. On the one hand, the in organello reconstitution led to conclusion that the transfer of two disulfide bonds is coupled to one Mia40-binding event, and, in contrast to the classic relay view, the involvement of Erv1 at this stage was proposed (Stojanovski *et al.*, 2008b). On the other hand, in vitro reconstitution experiments resulted in the conclusion that Mia40 alone is able to introduce both disulfide bonds into a substrate (Banci *et al.*, 2009, 2010; Bien *et al.*, 2010).

The relay mechanism excludes the direct association between a substrate and Erv1 in favor of bilateral interactions of Mia40–substrate and Mia40–Erv1. In contrast, an involvement of Erv1 implies the formation of a ternary complex of Mia40, substrate, and Erv1 (Stojanovski *et al.*, 2008b). In this work, we used an experimental design that allowed us to directly monitor the binding partners of IMS substrates and their dynamic changes. The use of saturating amounts of imported substrates and subsequent affinity purification from detergent lysed mitochondria provided evidence that oxidative biogenesis of the large group of IMS proteins representing both canonical classes of MIA substrates, twin CX_3C and CX_9C, requires a direct association of Erv1 in isolated mitochondria, as well as in vivo. Of interest, the engagement of Mia40 with the incoming substrate via its CPC motif is followed by Erv1 involvement. This initial engagement is followed by redox-conformational changes of the Mia40–substrate intermediate. These redox-conformational changes involve binding of Erv1 to the Mia40–substrate conjugate and ternary complex formation. For this binding, Erv1 uses an alternative site to the C2 region of Mia40, which is used for substrate binding and reoxidation of the CPC motif. The additional binding site and its role in the ternary complex were also proposed earlier based on the structure-driven dissection of Mia40 hydrophobic residues (Kawano *et al.*, 2009).

Although we have unambiguously shown the direct role of Erv1 in precursor oxidation at the stage of Mia40 binding, the mechanistic mode of ternary complex action is a subject of speculation. The proposed alternative site for Erv1 binding on Mia40 may serve disulfide bond channeling within a ternary complex. Given that our assays are based on the detection of noncovalent protein interactions, such interactions likely play an important role in this reaction. This is supported by the fact that we could not reproducibly see the ternary complex under denaturing and nonreducing conditions (Stojanovski *et al.*, 2008b). Our data are in agreement with the following mechanistic interpretations. A total of four electrons derived from a substrate are accepted in consecutive steps by Mia40 and Erv1 while in a ternary complex. After the oxidative biogenesis of an IMS substrate protein is complete, Mia40 is released, with the reduced CPC motif ready for the relay step (oxidation by Erv1), which sets Mia40 for the next round of precursor binding. How exactly the acceptance of four electrons via the ternary complex is achieved is not clear. On one hand, the cysteine residue analyses underline an important role for the C3–C6 couple, and on the other hand, redox-conformational changes of Mia40–substrate suggest the involvement of other cysteine residues of Mia40 in addition to C1 and C2 of the CPC motif. It is possible to envision that upon formation of the early Mia40–substrate intermediate the C3–C6 bond region in Mia40 becomes accessible to Erv1 binding. The nuclear magnetic resonance studies assigned the structural role for C3–C6 (Banci *et al.*, 2009), but Kawano *et al.* (2009) reported no change in the structure of Mia40 with C3 or C6 substitutions. This last observation, in combination with our mutational analysis, supports an alternative, nonstructural role for the C3 and C6 cysteine residues. Another possibility, that Erv1 may also be a direct donor of the substrate's second disulfide bond, cannot be excluded. In this case binding of substrate by Mia40 and its possible partial folding would be an important requirement for Erv1 action. It is worth noting that the IMS substrate proteins alone have not been reported to directly interact with Erv1. Furthermore, the *mia40-4* mutant accumulates more Mia40–Erv1 conjugate and is able to bind substrates efficiently but is defective in completion of oxidative folding (Chacinska *et al.*, 2004; Stojanovski *et al.*, 2008b). Thus Mia40 seems to play a central role in the complex, and a direct action of Erv1 on the IMS substrates is less likely. Finally, a possibility that Mia40 acts as a functional dimer, having the capacity to accept four electrons via its two CPC motifs, cannot be excluded. In this scenario, Erv1 would be involved in controlling an oligomeric state of Mia40 upon precursor binding. Further studies on the architecture of Mia40–Erv1 complexes will provide answers to these questions.

In summary, Erv1 plays an important role in oxidative biogenesis of the IMS proteins at two steps. Erv1 is not only responsible for reoxidation of the CPC motif of Mia40 after completion of an Mia40-mediated round of substrate oxidation, but it also participates in the stage of disulfide transfer, when the substrate is bound to Mia40,

forming the ternary complex. The Erv1 function at this step is to ensure that two disulfide bonds are transferred to the substrate without dissociation of single disulfide-bonded intermediate forms of the substrate from Mia40 into the IMS.

MATERIALS AND METHODS

Yeast strains and plasmid construction

YPH499 (*MAT*a, *ade2-101*, *his3-Δ200*, *leu2-Δ1*, *ura3-52*, *trp1-Δ63*, *lys2-801*; Sikorski and Hieter, 1989) was used as wild-type *Saccharomyces cerevisiae* strain in this study. The temperature-sensitive *mia40-3* (YPH-BG-fomp2-8), *mia40-4* (YPH-BG-fomp2-7), and *erv1-2int* mutants and strain harboring $Mia40_{Core}$ have been described previously (Chacinska *et al.*, 2004, 2008). To generate the cysteine residues mutants of Mia40, site-directed mutagenesis was performed, and the following plasmids based on the pFL39-MIA40 (BG8220) were constructed: BG9400 (C296S), BG9420 (C298S), BG9401 (C307S), BG9402 (C317S), BG9403 (C330S), and BG9446 (C340S). They were transformed into YPH499 *mia40*::*ADE2* containing pMIA40 (pGB8210; *URA3*-containing YEp352 with *MIA40*). pMIA40 was removed by plasmid shuffling upon 5-fluoroorotic acid treatment. The mutant strains produce Mia40 with the following amino acid residue substitutions: C296S (Mia40-C1S; 394), C307S (Mia40-C3S; 395), C317S (Mia40-C4S; 396), C330S (Mia40-C5S; 397), and C340S (Mia40-C6S; 402; Figure 1A). Strains with Mia40-C1S and Mia40-C3S versions lost functional mitochondrial DNA and became $rho^{0/-}$. For a comparison, wild-type strain and strain with Mia40-C6S (y486) were also made $rho^{0/-}$ upon treatment with ethidium bromide according to standard procedures. Strains coproducing wild-type Mia40 and $Mia40_{Core}$, $Mia40_{Core}$-C1S, or $Mia40_{Core}$-C2S were generated by transformation of YPH499 and *erv1-2int* (Chacinska *et al.*, 2008) with plasmids BG9334, BG9467, and BG9471, respectively. Oligonucleotide primers were designed to amplify from yeast genomic DNA the sequences coding for Pet191, Mic17, and Cox17. Each primer contained an additional extension encoding a restriction enzyme sequence. PCR products were restriction digested and inserted between *Not*I/*Eco*RI (for Pet191 and Mic17) or between *Not*I (for Cox17) sites in pESC-URA (Agilent, Santa Clara, CA). This procedure gave rise to the plasmids pAG1 (53), pAG2 (54), and pAG4 (56) encoding the fusion proteins Pet191, Mic17, and Cox17 each with a FLAG tag at their C-terminus. Wild-type YPH499 was transformed with the foregoing plasmids according to standard procedures.

Synthesis of precursor proteins

Radiolabeled Tim9 precursor protein was synthesized in rabbit reticulocyte lysate in the presence of [^{35}S]methionine and subjected to in organello import assays according to standard procedures (Stojanovski *et al.*, 2007) after precipitation with ammonium sulfate and denaturation in urea buffer (8 M urea, 30 mM 3-(*N*-morpholino) propanesulfonic acid [MOPS], pH 7.2, 10 mM DTT; Milenkovic *et al.*, 2009). The recombinant precursors were obtained according to the following procedure. *E. coli* strain BL21(DE3) was transformed with the plasmid pET10N-*TIM10* or pET10N-*TIM12* coding for *S. cerevisiae* Tim10 and Tim12 with a 10-histidine (His) tag at their N-terminus. The cells were grown in LBA medium (0.5% [wt/vol] yeast extract, 1% [wt/vol] bactopeptone, 0.5% [wt/vol] NaCl, 100 mg/l ampicillin) at 37°C to an $A_{600\ nm}$ of 1.0 and kept at 4°C overnight. A 10-ml culture was diluted 20-fold into LBA medium and grown to an $A_{600\ nm}$ of 0.5. To induce recombinant protein production, isopropyl-β-D(–)-thiogalactopyranoside was added to the culture to a final concentration of 1 mM and cells grown for 1–2 h. Cells were harvested by centrifugation, resuspended in sonication buffer (500 mM NaCl, 20 mM Tris, pH 8.0, 1 mM phenylmethylsulfonyl fluoride [PMSF], 0.1 μg/μl lysozyme, 0.5% [wt/vol] Triton X-100, 0.01 μg/μl DNase I, 1 mM $MgCl_2$, 50 mM DTT) before sonication on ice. After cell lysis and centrifugation to separate soluble and insoluble proteins, the recombinant proteins were purified on Ni-NTA agarose (Qiagen, Valencia, CA) either from the insoluble or from the soluble fraction under denaturing or native conditions, respectively. In the denaturing procedure, the insoluble protein material was solubilized in buffer A (8 M urea, 100 mM KH_2PO_4, 10 mM Tris, pH 8.0). After binding to the column and extensive washes in buffers B and C with decreasing pH (8 M urea, 100 mM KH_2PO_4, 10 mM Tris, 80 mM imidazole, pH 6.3–5.9), bound protein was eluted with elution buffer D (8 M urea, 100 mM KH_2PO_4, 10 mM Tris, pH 4.5), reduced by addition of 10 mM DTT, and then subjected to in organello import assays. In the native procedure, the cell lysis extract was loaded on the column and after washing with wash buffer A (500 mM NaCl, 20 mM Tris, pH 8.0) and buffer D (500 mM NaCl, 20 mM Tris, pH 8.0, 40 mM imidazole, 20 mM DTT), and bound proteins were eluted with the elution buffer (100 mM NaCl, 20 mM Tris, pH 8.0, 250 mM imidazole, 20 mM DTT, 20% [wt/vol] glycerol). Eluted proteins were denatured in urea buffer (8 M urea, 30 mM MOPS, pH 7.2, 10 mM DTT) and subjected to in organello import assays.

Mitochondrial procedures

Yeast were grown at 19–26°C on YPS medium (1% [wt/vol] yeast extract, 2% [wt/vol] bactopeptone, and 2% [wt/vol] sucrose) or YPG medium (1% [wt/vol] yeast extract, 2% [wt/vol] bactopeptone, and 3% [wt/vol] glycerol). Mitochondria were isolated by differential centrifugation according to the standard procedures (Meisinger *et al.*, 2006) and resuspend in SM buffer (250 mM sucrose, 10 mM MOPS-KOH, pH 7.2). The steady-state levels of mitochondrial proteins were analyzed by solubilization of samples in Laemmli buffer containing 50 mM DTT (reducing conditions) or 50 mM iodoacetamide (nonreducing conditions). Isolated mitochondria were also treated with increasing GSH concentrations (2–20 mM) for 5 min at 30°C in standard import buffer (250 mM sucrose, 80 mM KCl, 5 mM $MgCl_2$, 5 mM methionine, 10 mM KPi, 10 mM MOPS, pH 7.2), and the reaction was stopped by the addition of 50 mM iodoacetamide. Samples were washed with SM buffer (250 mM sucrose, 10 mM MOPS-KOH, pH 7.2) containing 50 mM iodoacetamide and analyzed by nonreducing SDS electrophoresis. Import of radiolabeled Tim9 or recombinant proteins, $Tim10_{His}$ (0.6–5 μg/50 μg mitochondrial protein) or $Tim12_{His}$ (0.45–1.35 μg/50 μg mitochondrial protein), into the isolated mitochondria was performed according to the standard procedures in standard import buffer at 25–30°C for 2–60 min. The volume of urea-denatured precursors did not exceed 2% of the import reaction. Import reactions were stopped by the addition of 50 mM iodoacetamide, followed by washing in SM buffer containing 50 mM iodoacetamide and analyzed by reducing or nonreducing SDS electrophoresis or by blue native electrophoresis followed by autoradiography. For the proteinase K sensitivity import assay, samples were incubated with 50 μg/ml proteinase K, followed by washing in SM buffer and analysis by SDS electrophoresis. The formation of intermediates between Mia40 and recombinant substrate proteins was analyzed under nonreducing conditions by immunodecoration with Mia40-specific antibody.

Affinity chromatography procedures

Recombinant $Tim10_{His}$ (2.0–2.5 μg/50 μg mitochondrial protein) was imported into mitochondria for 3–7 min at 15–25°C. The import reaction was stopped by the addition of 50 mM iodoacetamide. Mitochondria were isolated and solubilized in digitonin-containing

buffer (1% [wt/vol] digitonin, 10% [wt/vol] glycerol, 20 mM Tris-HCl, pH 7.4, 100 mM NaCl, 20 mM imidazole, pH 7.4, 50 mM iodoacetamide, and 1 mM PMSF) for 15 min on ice. After clarification by centrifugation, supernatants were incubated with Ni-NTA agarose (Qiagen) for 2 h at 4°C. Ni-NTA–bound material was washed two times in wash buffer (20 mM Tris, pH 7.4, 100 mM NaCl, 20 mM imidazole, pH 7.4) and eluted with elution buffer (20 mM Tris, pH 7.4, 100–200 mM NaCl, 400 mM imidazole, pH 7.4, and 50 mM iodoacetamide). Proteins were precipitated with StrataClean resin (Agilent) at 20°C for 15 min and analyzed by SDS electrophoresis, followed by Western blotting and immunodecoration.

Immunoaffinity purification of FLAG-fusion proteins

Wild-type YPH499 yeast transformed with plasmids pAG1, pAG2, and pAG4 were grown at 28°C on a selective medium without uracil and tryptophan with 2% (wt/vol) galactose overnight to induce expression of FLAG-fusion proteins. Yeast cells were harvested, resuspended in buffer F (20 mM Tris, pH 7.4, 300 mM NaCl, 50 mM iodoacetamide) and lysed by French press (CD-019 disruption system; Constant Cell, Kennesaw, GA) under pressure of 31 kpsi. Total extracts were further solubilized in digitonin-containing buffer (1% [wt/vol] digitonin, 20 mM Tris, pH 7.4, 300 mM NaCl, 50 mM iodoacetamide, 2 mM PMSF) for 15 min on ice. After clarification of the solubilized material, extracts were applied to Anti-FLAG M2 Affinity Gel (Sigma-Aldrich, St. Louis, MO) for 1.5 h at 4°C, followed by extensive washes with buffer F. Elution of the immunoprecipitated material was performed by incubation in Laemmli buffer with 50 mM DTT. The eluted extracts were analyzed by reducing SDS–PAGE, followed by Western blot.

Miscellaneous

SDS–PAGE was carried out according to standard procedures. Proteins were analyzed on 12.5 or 15% acrylamide gels. The blue native analysis and nonreducing SDS electrophoresis of imported Tim9 was performed as described previously (Chacinska *et al.*, 2004; Milenkovic *et al.*, 2009; von der Malsburg *et al.*, 2011). The gels were analyzed by digital autoradiography (Storm Imaging System; GE Healthcare, Piscataway, NJ) with the use of ImageQuant software. In some figures, nonrelevant gel parts were excised digitally. The Western blots were performed using polyvinylidene fluoride membranes (Millipore, Billerica, MA) and the enhanced chemiluminescence detection system. FLAG-fusion proteins were decorated with anti-FLAG M2 monoclonal antibodies raised in mouse (Stratagene, Santa Clara, CA). The chemiluminescence signals were detected with x-ray film (Foton-Bis, Bydgoszcz, Poland) or using digital system ImageQuant LAS4000 (GE Healthcare). In some gels, the position of molecular weight markers was determined from gel lanes run under the same conditions. Protein content was quantified according to the Bradford method using Roti-Quant (Carl Roth, Karlsruhe, Germany) and with bovine serum albumin as protein standard.

ACKNOWLEDGMENTS

We thank Nikolaus Pfanner and Diana Stojanovski for discussion. This work was supported by the Deutsche Forschungsgemeinschaft (Sonderforschungsbereich 746), the Foundation for Polish Science–Welcome Program cofinanced by the European Union within the European Regional Development Fund, an EMBO Installation grant, and a grant from Ministry of Science and Higher Education in Poland (N N301 298337; A.C.). In the course of this work A.G., T.C., and P.B. were supported by stipends within the Welcome program. K.N.T. is supported by an Australian Research Council Future Fellowship FT0992033.

REFERENCES

Arnesano F, Balatri E, Banci L, Bertini I, Winge DR (2005). Folding studies of Cox17 reveal an important interplay of cysteine oxidation and copper binding. Structure 13, 713–722.

Baker MJ, Webb CT, Stroud DA, Palmer CS, Frazier AE, Guiard B, Chacinska A, Gulbis JM, Ryan MT (2009). Structural and functional requirements for activity of the Tim9-Tim10 complex in mitochondrial protein import. Mol Biol Cell 20, 769–779.

Banci L, Bertini I, Calderone V, Cefaro C, Ciofi-Baffoni S, Gallo A, Kallergi E, Lionaki E, Pozidis C, Tokatlidis K (2011). Molecular recognition and substrate mimicry drive the electron-transfer process between MIA40 and ALR. Proc Natl Acad Sci USA 108, 4811–4816.

Banci L, Bertini I, Cefaro C, Cenacchi L, Ciofi-Baffoni S, Felli IC, Gallo A, Gonnelli L, Luchinat E, Sideris D, Tokatlidis K (2010). Molecular chaperone function of Mia40 triggers consecutive induced folding steps of the substrate in mitochondrial protein import. Proc Natl Acad Sci USA 107, 20190–20195.

Banci L, Bertini I, Cefaro C, Ciofi-Baffoni S, Gallo A, Martinelli M, Sideris DP, Katrakili N, Tokatlidis K (2009). MIA40 is an oxidoreductase that catalyzes oxidative protein folding in mitochondria. Nat Struct Mol Biol 16, 198–206.

Bien M, Longen S, Wagener N, Chwalla I, Herrmann JM, Riemer J (2010). Mitochondrial disulfide bond formation is driven by intersubunit electron transfer in Erv1 and proofread by glutathione. Mol Cell 37, 516–528.

Bulleid NJ, Ellgaard L (2011). Multiple ways to make disulfides. Trends Biochem Sci 36, 485–492.

Chacinska A, Guiard B, Müller JM, Schulze-Specking A, Gabriel K, Kutik S, Pfanner N (2008). Mitochondrial biogenesis, switching the sorting pathway of the intermembrane space receptor Mia40. J Biol Chem 283, 29723–29729.

Chacinska A, Koehler CM, Milenkovic D, Lithgow T, Pfanner N (2009). Importing mitochondrial proteins: machineries and mechanisms. Cell 138, 628–644.

Chacinska A, Pfannschmidt S, Wiedemann N, Kozjak V, Sanjuán Szklarz LK, Schulze-Specking A, Truscott KN, Guiard B, Meisinger C, Pfanner N (2004). Essential role of Mia40 in import and assembly of mitochondrial intermembrane space proteins. EMBO J 23, 3735–3746.

Daithankar VN, Farrell SR, Thorpe C (2009). Augmenter of liver regeneration: substrate specificity of a flavin-dependent oxidoreductase from the mitochondrial intermembrane space. Biochemistry 48, 4828–4837.

Depuydt M, Messens J, Collet JF (2011). How proteins form disulfide bonds. Antioxid Redox Signal 15, 49–66.

Dolezal P, Likic V, Tachezy J, Lithgow T (2006). Evolution of the molecular machines for protein import into mitochondria. Science 313, 314–318.

Gabriel K, Milenkovic D, Chacinska A, Müller JM, Guiard B, Pfanner N, Meisinger C (2007). Novel mitochondrial intermembrane space proteins as substrates of the MIA import pathway. J Mol Biol 365, 612–620.

Grumbt B, Stroobant V, Terziyska N, Israel L, Hell K (2007). Functional characterization of Mia40p, the central component of the disulfide relay system of the mitochondrial intermembrane space. J Biol Chem 282, 37461–37470.

Hell K (2008). The Erv1-Mia40 disulfide relay system in the intermembrane space of mitochondria. Biochim Biophys Acta 1783, 601–609.

Kawano S, Yamano K, Naoé M, Momose T, Terao K, Nishikawa S, Watanabe N, Endo T (2009). Structural basis of yeast Tim40/Mia40 as an oxidative translocator in the mitochondrial intermembrane space. Proc Natl Acad Sci USA 106, 14403–14407.

Khalimonchuk O, Winge DR (2008). Function and redox state of mitochondrial localized cysteine-rich proteins important in the assembly of cytochrome c oxidase. Biochim Biophys Acta 1783, 618–628.

Koehler CM (2004). The small Tim proteins and the twin CX_3C motif. Trends Biochem Sci 29, 1–4.

Kurz M, Martin H, Rassow J, Pfanner N, Ryan MT (1999). Biogenesis of Tim proteins of the mitochondrial carrier import pathway: differential targeting mechanisms and crossing over with the main import pathway. Mol Biol Cell 10, 2461–2474.

Longen S, Bien M, Bihlmaier K, Kloeppel C, Kauff F, Hammermeister M, Westermann B, Herrmann JM, Riemer J (2009). Systematic analysis of the twin CX_9C protein family. J Mol Biol 393, 356–368.

Lutz T, Neupert W, Herrmann JM (2003). Import of small Tim proteins into the mitochondrial intermembrane space. EMBO J 22, 4400–4408.

Meisinger C, Wiedemann N, Rissler M, Strub A, Milenkovic D, Schönfisch B, Müller H, Kozjak V, Pfanner N (2006). Mitochondrial protein sorting: differentiation of beta-barrel assembly by Tom7-mediated segregation of Mdm10. J Biol Chem 281, 22819–22826.

Mesecke N, Terziyska N, Kozany C, Baumann F, Neupert W, Hell K, Herrmann JM (2005). A disulfide relay system in the intermembrane space of mitochondria that mediates protein import. Cell 121, 1059–1069.
Milenkovic D, Ramming T, Müller JM, Wenz LS, Gebert N, Schulze-Specking A, Stojanovski D, Rospert S, Chacinska A (2009). Identification of the signal directing Tim9 and Tim10 into the intermembrane space of mitochondria. Mol Biol Cell 20, 2530–2539.
Müller JM, Milenkovic D, Guiard B, Pfanner N, Chacinska A (2008). Precursor oxidation by Mia40 and Erv1 promotes vectorial transport of proteins into the mitochondrial intermembrane space. Mol Biol Cell 19, 226–236.
Naoé M, Ohwa Y, Ishikawa D, Ohshima C, Nishikawa S, Yamamoto H, Endo T (2004). Identification of Tim40 that mediates protein sorting to the mitochondrial intermembrane space. J Biol Chem 279, 47815–47821.
Neupert W, Herrmann JM (2007). Translocation of proteins into mitochondria. Annu Rev Biochem 76, 723–749.
Riemer J, Bulleid N, Herrmann JM (2009). Disulfide formation in the ER and mitochondria: two solutions to a common process. Science 324, 1284–1287.
Sato Y, Inaba K (2012). Disulfide bond formation network in the biological kingdoms. FEBS J 279, 2262–2271.
Sideris DP, Petrakis N, Katrakili N, Mikropoulou D, Gallo A, Ciofi-Baffoni S, Banci L, Bertini I, Tokatlidis K (2009). A novel intermembrane space-targeting signal docks cysteines onto Mia40 during mitochondrial oxidative folding. J Cell Biol 187, 1007–1022.
Sideris DP, Tokatlidis K (2010). Oxidative protein folding in the mitochondrial intermembrane space. Antioxid Redox Signal 13, 1189–1204.
Sikorski RS, Hieter P (1989). A system of shuttle vectors and yeast host strains designed for efficient manipulation of DNA in *Saccharomyces cerevisiae*. Genetics 122, 19–27.
Stojanovski D, Guiard B, Kozjak-Pavlovic V, Pfanner N, Meisinger C (2007). Alternative function for the mitochondrial SAM complex in biogenesis of alpha-helical TOM proteins. J Cell Biol 179, 881–893.
Stojanovski D, Milenkovic D, Müller JM, Gabriel K, Schulze-Specking A, Baker MJ, Ryan MT, Guiard B, Pfanner N, Chacinska A (2008b). Mitochondrial protein import: precursor oxidation in a ternary complex with disulfide carrier and sulfhydryl oxidase. J Cell Biol 183, 195–202.
Stojanovski D, Müller JM, Milenkovic D, Guiard B, Pfanner N, Chacinska A (2008a). The MIA system for protein import into the mitochondrial intermembrane space. Biochim Biophys Acta 1783, 610–617.
Terziyska N, Grumbt B, Kozany C, Hell K (2009). Structural and functional roles of the conserved cysteine residues of the redox-regulated import receptor Mia40 in the intermembrane space of mitochondria. J Biol Chem 284, 1353–1363.
Terziyska N, Lutz T, Kozany C, Mokranjac D, Mesecke N, Neupert W, Herrmann JM, Hell K (2005). Mia40, a novel factor for protein import into the intermembrane space of mitochondria is able to bind metal ions. FEBS Lett 579, 179–184.
Tienson HL, Dabir DV, Neal SE, Loo R, Hasson SA, Boontheung P, Kim SK, Loo JA, Koehler CM (2009). Reconstitution of the Mia40-Erv1 oxidative folding pathway for the small Tim proteins. Mol Biol Cell 20, 3481–3490.
von der Malsburg K *et al*. (2011). Dual role of mitofilin in mitochondrial membrane organization and protein biogenesis. Dev Cell 21, 694–707.
Webb CT, Gorman MA, Lazarou M, Ryan MT, Gulbis JM (2006). Crystal structure of the mitochondrial chaperone TIM9.10 reveals a six-bladed alpha-propeller. Mol Cell 21, 123–133.